An Automatic Weak Learner Formulation for Lithium-ion Battery State of Health Estimation

Meng, Jinhao; Cai, Lei; Stroe, Daniel-Ioan; Huang, Xinrong; Peng, Jichang; Liu, Tianqi; Teodorescu, Remus

Published in:
I E E E Transactions on Industrial Electronics

DOI (link to publication from Publisher):
10.1109/TIE.2021.3065594

Publication date:
2022

Document Version
Accepted author manuscript, peer reviewed version

An Automatic Weak Learner Formulation for Lithium-ion Battery State of Health Estimation

Jinhao Meng, *Member, IEEE*, Lei Cai, Daniel-Ioan Stroe, *Member, IEEE*, Xinrong Huang, *Student Member, IEEE*, Jichang Peng, Tianqi Liu, and Remus Teodorescu, *Fellow, IEEE*

***Abstract*—Current pulses are convenient to be actively implemented by a Battery Management System (BMS). However, the Short-Term Features (STF) from current pulses originate from various sensors with uneven qualities, which hinders one powerful and strong learner with STF for the battery SOH estimation. This paper thus proposes an optimized weak learner formulation procedure for Lithium-ion (Li-ion) battery SOH estimation, which further enables the automatic initialization and integration of the weak learners with STF into an efficient SOH estimation framework. A Pareto Front-based Selection Strategy (PFSS) is designed to select the representative solutions from the non-dominated solutions fed by a Knee point driven Evolutionary Algorithm (KnEA), which guarantees both the diversity and accuracy of the weak learners. Afterwards, the weak learners, whose coefficients are obtained by Self-adaptive Differential Evolution (SaDE), are integrated by a weight-based structure. The proposed method utilizes the weak learners with STF to boost the overall performance of SOH estimation. The validation of the proposed method is proved by $LiFePO_4$/C batteries under accelerated cycling ageing test including one mission profile providing Primary Frequency Regulation (PFR) service to the grid and one constant current profile.**

***Index Terms*—Lithium-ion battery; State of health estimation; Automatic weak learner formulation; Ensemble learning.**

I. Introduction

RENEWable energy has recently played a significant role in the power supply as well as in the transportation sector. For improving the flexibility and reliability of the energy flow in the electrical grid and the driving range in e-mobility, batteries have become a key energy storage technology [1]–[4]. Lithium-ion (Li-ion) batteries have drawn much attention from academia and industry due to their superior performance, such as high energy density, long life-span, low maintenance, *etc.* [5]–[9]. However, the complex and uncertain degradation behavior of Li-ion batteries still hinders their applications in a large-scale system [10]. During the long-time operation, the performance of the Li-ion battery is subject to degradation resulting in capacity fading and increased internal resistance. Thus, the capacity and internal resistance can be used to express the State of Health (SOH) of the batteries. The battery degradation is influenced by various factors, such as temperature, current rate, cycling number, *etc*.

Accurate SOH estimation can ensure the reliable and economically viable operations of the battery by managing its lifespan [11]. In this way, the aged batteries can be replaced before causing any severe accidents. The long downtime periods can be avoided so that the usage of the battery could be maximized. Unfortunately, the SOH cannot be directly measured by placing a sensor inside the battery. Measuring the capacity or internal resistance is a straightforward approach to know battery SOH. However, the Li-ion battery is not always fully charged or discharged during the operation, which means it is not convenient to measure its capacity during daily usage. Considering the fact that the internal resistance of a high-power Li-ion battery is usually a small value in the range of milli-Ohms, it is also not effective to measure an accurate internal resistance taking into account the interference from the sensors. Thus, various advanced techniques have been proposed to estimate the battery SOH.

The existing battery SOH estimation methods in literature can be divided into three categories: empirical models [12], model-based methods [13], [14], and data-driven methods [15]–[17]. After collecting the measurement from a long-term degradation test under various stresses, such as storage time, temperature, cycling current rate, empirical models are developed based on the polynomial or exponential functions to describe the connections between those stresses and the battery SOH [18]. One drawback of the empirical model is that the models are only suitable for a specific battery for which they are parameterized. The main limitations are the model's oversimplified structure and the developer's personal experiences [19]. Model-based estimation identifies the internal resistance and capacity online [13]. It is noted that the online estimation of resistance and capacity is vulnerable.

This work was supported by the Fundamental Research Funds for the Central Universities under Grant YJ202013, and the China Postdoctoral Science Foundation under Grant 2020M673218, and the Fund of Robot Technology Used for Special Environment Key Laboratory of Sichuan Province under Grant 20KFKT02, and National Natural Science Foundation of China under Grant 61973042, and the Natural Science Basic Research Plan in Shaanxi Province of China under Grant 2019JQ-746.

J. Meng and T. Liu are with the College of Electrical Engineering, Sichuan University, Chengdu 610065, China (e-mail: scmjh2008@163.com; tqliu@scu.edu.cn).

L. Cai is both with the Faculty of Computer Science and Engineering, Xi'an University of Technology, Xi'an 710048, China, and Shaanxi Key Laboratory for Network Computing and Security Technology, Xi'an 710048, China (e-mail: caileid@gmail.com).

D. Stroe, X. Huang and R. Teodorescu are with the Department of Energy Technology, Aalborg University, Aalborg 9220, Denmark (e-mails: dis@et.aau.dk; hxi@et.aau.dk; ret@et.aau.dk).

J. Peng is with the Smart Grid Research Institute, Nanjing Institute of Technology, Nanjing 211167, China (email: linkpjc@gmail.com).

The identified values are easily contaminated by noises from the sensors [20]. In addition, the state space equations for internal resistance and capacity identification are not explicit. For example, online capacity identification usually needs the battery State of Charge (SOC) acting as an input, but the SOC itself is an estimated value with uncertainties.

Recently, great progress has been made in the machine learning area, which utilizes the information behind the original dataset. Machine learning techniques, such as Extreme Learning Machine (ELM) [21], Gaussian Process Regression (GPR) [16], [22], Support Vector Regression (SVR) [15], [17], [23], [24], Prior Knowledge-based Neural Network (PKNN) [25], Long Short-Term Memory (LSTM) network [26], *etc.*, have been used for SOH estimation. An efficient SVR based SOH estimation method under different measurement conditions is established in [15], which aims at improving the flexibility of using one data-driven estimator in reality. After selecting the degradation features from the voltage curve, the Markov chain is adopted to enhance the performance of PKNN-based SOH estimator in a long-term period [25]. Using LSTM as the base model, transfer learning is chosen to estimate the battery SOH in [26] with the features coming from the charging voltage curves.

After analyzing the previous works, we find there are two pivotal procedures for battery SOH estimation with data-driven methods: the feature collection and the training process. The feature contains information related to battery ageing, and a training process is used to establish the data-driven methods. In [27]–[30], the long-term degradation features extracted from Incremental Capacity (IC) curve and Differential Voltage (DV) curve are used. It is easily known from the calculation of the IC and DV curves that those curves are sensitive to the measurement noise. Additionally, the battery has to be charged or discharged with an extremely small current (1/25C) [31] for the purpose of acquiring the IC and DV curves in reality. The aforementioned limitations restrict the usage of IC and DV curve-based methods. The voltage curve during the charging process is chosen as the features in [32]–[34]. Although the charging process is relatively deterministic, the degradation features from the voltage charging curve are still subjected to a long-term measurement period. One should be aware that the users may not always charge the battery through a pre-defined voltage range only for SOH estimation. Thereby, one issue for the data-driven methods in battery SOH estimation is that the feature cannot be conveniently obtained in real applications.

Another issue is that we can obtain only weak learners, which are not perfect, in most conditions. Although the data-driven methods have great potential in the field of SOH prediction [35], [36], we find that most of the algorithms attempt to establish a strong estimator. In fact, it is quite difficult to establish a perfect estimator in practice. The historical dataset of the battery comes from defective sensors, and the quality of the measurement is difficult to be unified. In addition, the training samples cannot cover all the cycling conditions of a specific scenario, and it is burdensome to set a group of right hyper-parameters for training a data-driven method.

In order to mitigate the above issues, we propose an ensemble learning framework for Li-ion battery SOH estimation with weak learners fed by Short-Term Features (STF). Those STFs come from current pulse lasting only a few seconds, which is convenient to be actively imposed to the cells in real-life applications. Therefore, the first issue regarding the convenience of the feature is alleviated. Considering the fact that only weak learners with the defective dataset and the imperfect hyper-parameters are the reality for SOH estimation in real-life, an automatic weak learner formulation procedure combined with an ensemble framework, is proposed to solve the second issue on estimation accuracy. Ensemble framework can boost the overall SOH estimation performance by integrating a group of weak learners, which can only predict the battery SOH with limited ability. The weak learners should be as diverse as possible in an ensemble learning framework [37]. Thus, a Pareto Front-based Selection Strategy (PFSS) is proposed to find the representative solutions originated from the Knee point driven Evolutionary Algorithm (KnEA). Afterwards, the integration of weak learners is optimized by Self-adaptive Differential Evolution (SaDE) for the ultimate estimation.

The main contributions of this work are as follows:

(1) An automatic weak learner formulation procedure is proposed for battery SOH estimation by combining a PFSS with the non-dominated solutions generated by KnEA. In this way, the diversity of each weak learner is naturally guaranteed for an efficient ensemble estimator.
(2) STFs from the current pulses, which are easy to be obtained in real-life applications, are chosen as the features for battery SOH estimation.
(3) SaDE, which avoids the time-consuming parameter tuning process in traditional Differential Evolution (DE), is used to integrate all the weak learners so that the predictability of SOH estimator can be significantly improved.
(4) Five $LiFePO_4$/C (LFP/C) batteries aged under two different cycling conditions, including one mission profile providing the Primary Frequency Regulation (PFR) service to the grid and one constant current profile, are used to verify the proposed method.

The rest of the paper is organized as follows. Section II describes the STF. The automatic weak learner formulation and the proposed ensemble framework are detailed in Section III. The validation of the proposed method is presented in Section IV. Conclusions are given in Section V.

II. The short-term feature for Li-ion battery SOH estimation

Data-driven methods have great potential in battery SOH estimation [36]. Features containing valuable information related to battery ageing should, however, be properly chosen in advance.

The procedure in Fig. 1 is designed for cycling the five LFP/C batteries under two different scenarios. For Case 1, two LFP/C batteries are cycled with a mission profile, which corresponds to a battery energy storage system providing PFR to the grid. The mission profile has a length of one week, and the SOC varies between 10% and 90%. In Case 2, a constant current I=10A (4C-rate) is used for cycling three LFP/C batteries in the range from 20% to 80% SOC.The ageing test is

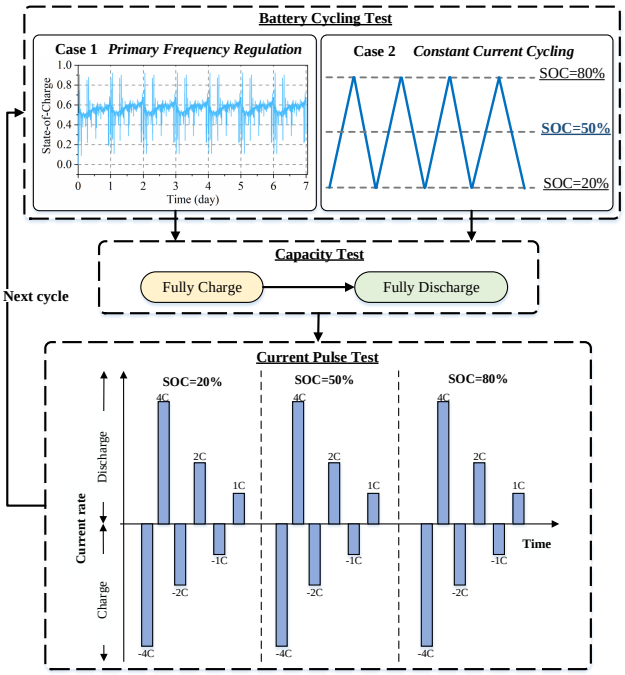

Fig. 1. The test procedure

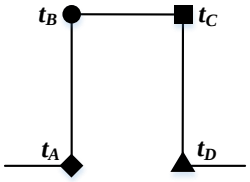

Fig. 2. The current pulse

periodically stopped and a Reference Performance Test (RPT), including capacity test and current pulse test, is performed. The current pulse test includes a series of charging and discharging current pulses under three different C-rates (1C, 2C, 4C) at SOCs (20%, 50%, 80%). Each current pulse lasts 18 seconds. During the ageing test, the batteries are placed in the climatic chamber at 25^{o}C for Case 1 and 42.5^{o}C for Case 2. The measurement data is logged with 1-second resolution. The specifications of the LFP/C battery are as follows: the nominal capacity is 2.5Ah, and the voltage ranges from 2.0V to 3.6V. More information related to the LFP/C battery can be found in [17].

For clarifying the STFs, the pattern of the current pulse is illustrated in Fig. 2. It can be seen that the current profile changes at 4 different transition times, *i.e.*, t_A, t_B, t_C, t_D. The voltage responses of a LFP/C battery measured at SOC = 20% and $I = 10$A are chosen as an example in Fig. 3. Since the voltage curves vary from Week 1 to Week 33, those voltage responses definitely contain the information related to the battery degradation. For simplicity, the voltage values at 4 transfer moments (t_A, t_B, t_C, t_D) is chosen as the features and are represented as a vector $[U_A, U_B, U_C, U_D]$. As shown in Fig. 1, the current pulse is performed at 18 different conditions.

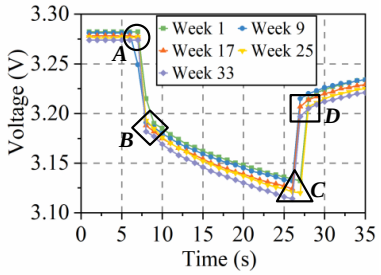

Fig. 3. The voltage response of the current pulse test (SOC=20%, I=10A) at different ageing stages

Thus, we have altogether a 72-dimension vector acting as the input of the weak learners in the training phase. Because the current pulse lasts only 18 seconds and the transfer moments have already known from the controller of the power converter, the proposed feature is very convenient to be obtained in real applications. Features under various conditions have the necessary diversity, which can lead to a promotion in the generalization of the ensemble learning framework. Thus, the diversity of the weak learners can be firstly achieved by the proposed feature to some extent.

III. The Proposed SOH Estimation Method

Although STFs are efficient in practical applications, they are also fragile considering the measurement noise. Thus, only weak learners with limited accuracy can be obtained in reality. The main purpose of this work is to optimize the weak learner formulation with good diversity so that the weak learners can be utilized to boost the overall performance of the SOH estimation through an ensemble framework.

The diversity of weaker learners must be guaranteed at first. Although different voltage responses can naturally ensure the diversity of the weak learners to some extent, we still need to enhance the diversity in the phase of the weak learner formulation. Moreover, we aim at creating a genetic method without the requirement of any manual interactions on the feature selection and configuration of the algorithm. The procedure of the SOH estimation method is shown in Fig. 4.

In Step 1, the process of feature selection and hyperparameters tuning are formed as a Multi-objective Optimization Problem (MOP) which considers both the accuracy and the complexity. The expected solutions are non-dominated with each other and well-distributed in the objective space of MOP, which means the solutions have the property of diversity. Thanks to the natural diversity of the non-dominated solutions from MOP, the requirement of diversity for ensemble learning can be guaranteed simultaneously. However, it is still very challenging to solve this MOP, especially in the scenario where the diversity is more preferable. Hence, KnEA [38] is utilized, which makes full use of its advantage on diversity first and convergence second strategy. The ultimate solutions are selected from KnEA according to the shape of the Pareto front, which can be summarized as PFSS in this work.

In Step 2, Support Vector Regression (SVR) is chosen to train the optimized weak learners, which can generate the

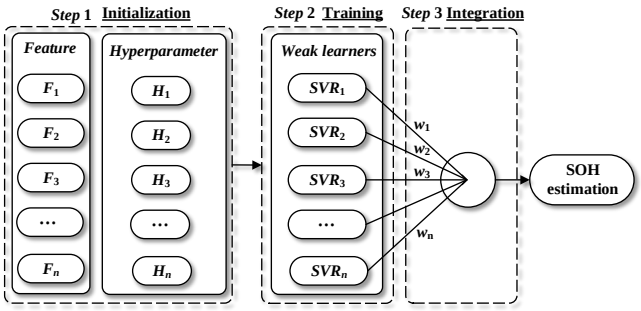

Fig. 4. The procedure of the proposed method

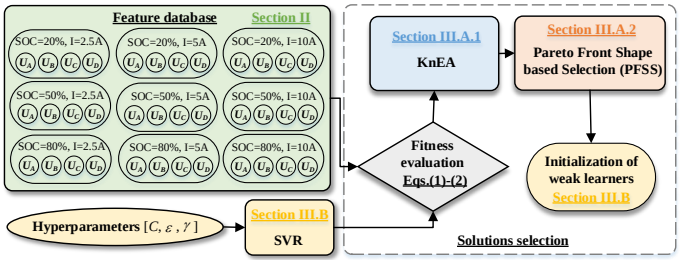

Fig. 6. The procedure of the optimized weak learner formulation

regression model with good generalization to unknown dataset taking the advantages of the Vapnik-Chervonenkis (VC) and statistical theory.

Afterwards, a weight coefficient-based structure with SaDE is used to integrate the weak learners into one unified framework in Step 3, which avoids the costly trial and error procedure on the trial vector generation strategies and tuning the associate parameters in traditional DE [39].

A. Automatic weak learner formulation

In order to finalize the automatic weak learner formulation, the selection of the STF and the hyperparameters of SVR are formulated as an optimization problem.

In feature selection, the measurements come from various conditions in reality. Especially, the current pulses used in this work are convenient yet fragile. The overall quality of the STF is hard to be unified and guaranteed in a BMS. 72 dimensions STF has to be carefully selected to extract useful information. Thus, the procedure of feature selection is formed as a combinatorial optimization problem in this work. The decision value for each feature is a binary value that specifies whether the current feature is selected or not as shown in Fig. 5.

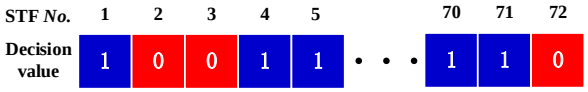

Fig. 5. The decision value for each feature

Besides the STFs, tuning the hyperparameters of SVR is another aspect to improve the diversity of the weak learners. SVR depends on the hyperparameters C, ϵ and γ in the training phase. Thus, the hyperparameters of SVR should be tuned not only to improve the performance of the weak learners but also to enhance their diversity from the training aspect. The main idea of synchronously optimizing the feature and hyperparameters can be referred to [17].

This work optimizes the feature selection and the model setting simultaneously through a MOP procedure. For a specific weak learner, we generally tend to use all 72 dimensions STFs hoping that sufficient information can be included. But large numbers of STFs need the measurement from various conditions and also induce a higher computing burden. In addition, the STF contains noise and redundancy, which will lower the performance of the weak learner. There sometimes exists a conflict, that is, to minimize the number of the features and to maximize the accuracy of the weak learners. Hence, the first reason that we formulate the MOP is to balance the two objectives for obtaining accurate and efficient weak learners. Another pivotal reason is to utilize its basic property that the diversity of the weak learner will naturally be fulfilled once the MOP is solved. The main idea of MOP for feature selection and hyperparameters tuning can be found in [15]. Specifically, the two objectives are defined as follows,

$$f_1 = MSE_{5-foldCV}(SVR) \tag{1}$$

$$f_2 = Num_{feature} \tag{2}$$

where $MSE_{5-foldCV}$ is the MSE of SVR under 5-fold cross-validation, $Num_{feature}$ is the number of the features. It should be noted that $Num_{feature}$ counts $[U_A, U_B, U_C, U_D]$ individually in this work.

KnEA is used to solve the MOP and generates diverse non-dominated solutions as shown in Fig. 6. According to the two objectives in Eqs.(1) and (2), KnEA will select features from the database as well as tuning the hyperparameters of SVR in each iteration. Once the criterion of KnEA is meet, we will obtain the non-dominated solutions for the MOP. Then, PFSS will take over to choose representative solutions with good diversity. By using KnEA to solve the MOP and PFSS to choose a few representative solutions, the weak learners are automatically initialized. More details related to KnEA and the proposed PFSS will be detailed as follows.

1) *KnEA* [38]: Knee points are preferred for the selection of the non-dominated solutions in MOP. KnEA uses the knee points from the current population acting as the secondary criterion for the parents' generation. To be more specific, the solutions are firstly chosen according to the dominance comparison. If two solutions are non-dominated with each other, the knee point will be used as the secondary criterion.

The knee point is chosen only if one solution has the largest distance to the extreme line in the nearest neighborhood. The extreme line L is determined by the solutions that have the maximum value of the cost functions f_1 and f_2. For example, the a_1 and a_5 in Fig.7. Define that L is represented by the function $ax + by + c = 0$. The distance of the solution a_3 can be calculated by the following equation,

$$d(a_3, L) = \frac{|ax_3 + by_3 + c|}{\sqrt{a^2 + b^2}} \tag{3}$$

where x_3 and y_3 are the coordinates of a_3. According to the largest distance from Eq. (3), a_3 is thus knee point in Fig.7.

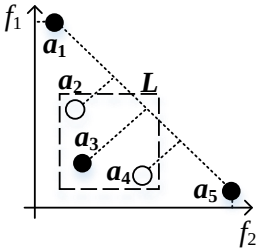

Fig. 7. The knee point selection in KnEA

From the above descriptions, we can see that the non-dominated solutions with knee point selection can also speed up the convergence of the optimization for a MOP. If the neighbourhood relationship of the non-dominated solution can be maintained properly, the diversity will also be satisfied. In KnEA, the size of the neighbourhood of the solutions is adaptively adjusted so that the survived knee points would be well sampled in the whole objective space. Thus, with high speed on convergence and good property on diversity, KnEA can provide us with a series of solutions that have a high quality of diversity.

2) Pareto front based selection strategy (PFSS): Currently, we cannot pass the optimized solutions directly to the integration steps. The main concern now is how to determine a specific number of solutions in advance. In this phase, we need strong diversification whereas no strong convergence is needed. Therefore, a PFSS procedure is proposed to choose a few representative solutions according to the shape of the Pareto front. In this way, the diversity of the weak learners is preserved to the utmost extent, and the numbers of weak learners can be reduced.

The pseudo-code of the PFSS is shown in Algorithm 1. Lines 2 and 3 are used to select a boundary solution from the current solution set. The purpose of loop between Lines 5 and 9 is to iteratively select a solution from the final population of KnEA with the largest angle to the $\mathbf{V}$. It is worth mentioning that the angle of a solution vector to a set can be defined as the smallest one among the angles between this solution and all solutions,

$$angle(\mathbf{s}, \mathbf{V}) = \arg \min_{\mathbf{v_i} \in \mathbf{V}} < \mathbf{s}, \mathbf{v}_i > \tag{4}$$

At last, a solution set $\mathbf{V}$ with K solutions is returned.

Fig. 8 is an example for clarifying the PFSS. The angle of a vector to $\mathbf{S}$ is defined as the smallest angle between the vector and the rest vectors in $\mathbf{S}$. $\mathbf{s}_r$ is randomly selected as the first vector. Then, $\mathbf{s}_1$ has the largest angle to $\mathbf{s}_r$, and $\mathbf{s}_2$ has the largest angle to $\mathbf{s}_1$. $\mathbf{s}_3$ has the largest angle to $\mathbf{S}$ including $\mathbf{s}_1$ and $\mathbf{s}_2$. If three solutions are the target, the red arrows in Fig. 8 will be the selected solutions by PFSS.

B. Training the weak learners

After the automatic weak learner formulation, each solution has already contained the suitable hyperparameters and STFs for initializing the SVR based weak learners.

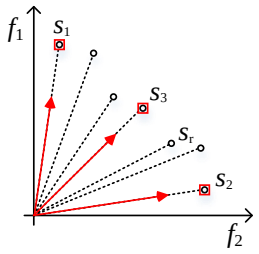

Fig. 8. Example of the PFSS

Algorithm 1 Update procedure of PFSS

Input: Solution set $\mathbf{S}$, the size of selected solution K, the number of solution set N

1: $\mathbf{V} = \emptyset$
2: $p \leftarrow$ rand(1, N) // To randomly select an index of solution from the solution set
3: $\mathbf{V}$ = $\mathbf{V}$ $\cup\{\mathbf{s}_p\}$, $\mathbf{S}$ = $\mathbf{S}\backslash\{\mathbf{s}_p\}$
4: $i \leftarrow 0$
5: **while** $i < K - 1$ **do**
6: Find a solution $\mathbf{s}_j$ in $\mathbf{S}$ with the largest angle to $\mathbf{V}$. An angle of the solution to a set can refer to Eq. (4)
7: $\mathbf{V}$ = $\mathbf{V}$ $\cup\{\mathbf{s}_j\}$, $\mathbf{S}$ = $\mathbf{S}\backslash\{\mathbf{s}_j\}$
8: $i++$
9: **end while**
10: **return** $\mathbf{V}$

Compared with other regression algorithms, SVR has a strictly proof in mathematics and can be represented as follows,

$$f(\mathbf{x}) = \mathbf{w}^T \cdot \varphi(\mathbf{x}) + b \tag{5}$$

where $\mathbf{w}$ and b are the coefficients to be adjusted.

The original SVR can be transferred to solve the following optimization problem,

$$\min \frac{1}{2}\|\mathbf{w}\|^2 + C\sum_{i=1}^{N}(\xi_i + \xi_i^*) \tag{6}$$

Subject to the constrains,

$$\begin{cases} y_i - \mathbf{w}^T \cdot \varphi(\mathbf{x}_i) - b \le \varepsilon + \xi_i \\ \mathbf{w}^T \cdot \varphi(\mathbf{x}_i) + b - y_i \le \varepsilon + \xi_i^* \\ \xi_i, \xi_i^* \ge 0 \end{cases} \tag{7}$$

where C is a positive constant and ξ_i is the slack variable.

After solving the above quadratic optimization, the SVR regression function can be reformulated as follows,

$$f(\mathbf{x}) = \sum_{i=1}^{N}(\beta_i^* - \beta_i) \cdot K(\mathbf{x}_i, \mathbf{x}) + b \tag{8}$$

where β_i is the Lagrangian multipliers, and $K(\mathbf{x}_i, \mathbf{x})$ is the kernel function.

The kernel function can convert the nonlinear space into a higher dimensional space. It is noted that the RBF kernel function is able to approximate other kernel functions by tuning its parameters. Thus, we choose to use the RBF kernel function, which can be expressed as follows,

$$K(\mathbf{x}_i, \mathbf{x}_j) = \exp(-\frac{1}{2}\|\mathbf{x}_i - \mathbf{x}_j\|^2/\gamma) \tag{9}$$

From the above equations, we can find that C (Eq. (6)) controls the trade-off between the flatness of SVR and the degree to which the deviation larger than ϵ is tolerated, and γ determines the performance of the kernel function. C, ϵ and γ can significantly influence the performance of SVR. Thus, it is possible to control the diversity of weak learners by tuning the hyperparameters of SVR. Due to the superior performance and the feasibility of controlling the diversity, SVR is chosen in this work to form the weak learners.

C. Integration of the weak learners

Finally, the weak learners are integrated into an ensemble framework as shown in step 3 of Fig. 4 for the SOH estimation. The weak learners with STF are integrated by a weight coefficients-based structure with SaDE [39]. A proper set of the weight coefficients $(w_1, w_2, w_3, \dots)$ can be obtained by SaDE. The cost function of SaDE is defined as the MSE of the SOH estimation with 5-fold cross-validation in this work, which is similar to Eq. (1).

The performance of traditional DE is closely related to the strategy for generating the trial vectors and the control parameters, such as the population size *NP*, the scaling factor *F*, and the crossover rate *CR*. In order to achieve good solutions, a suitable trial vector generation strategy and the control parameters for a specific problem have to be chosen for DE. Thus, traditional DE still suffers from a time-consuming tuning process. To alleviate this issue, SaDE is used to adaptively adjust the trial vector generation strategy and the associated parameters. A candidate pool including several typical strategies in SaDE enables the adaptively choosing of a suitable generation strategy for the trial vector. According to the memory of success and failure, the strategic probability is learned from the success rate of a particular strategy. Moreover, *CR* is generated from a normal distribution *N(CRm, Std)*, and *CRm* can be adjusted according to the experiences of *CR* in the previously promising solutions. The scaling factor *F*, related to the convergence speed, can be randomly selected in another normal distribution *N*(0.5,0.3). In this way, the trial and error tuning process is avoided in SaDE, which is capable of guaranteeing high-quality solutions in different situations. For more details about SaDE, please refer to [39].

IV. Experimental Validation

In this work, 5 LFP/C batteries are aged with different cycling profiles as shown in Fig. 1. FuelCon test station is used to implement the battery degradation test as introduced in [24]. After the long-term cycling test, the capacity variations of the 5 cells are shown in Fig. 9 and Table. I.

A. Validation of the automatic weak learner formulation

An optimized formulation procedure is responsible for the automatic initialization of the weak learners with good diversity, which is critical to the overall performance of the SOH estimation in this work. Thus, the diversity of the weak learner is firstly validated in this subsection.

According to the two cost functions (Eqs. (1) and (2)), the non-dominated solutions from KnEA are illustrated as

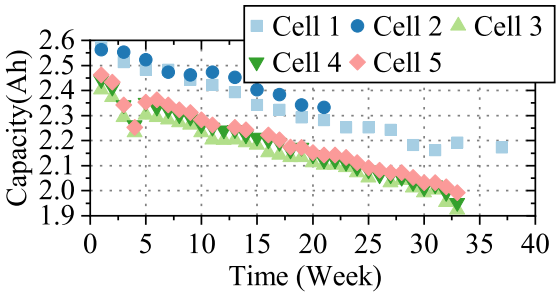

Fig. 9. The variation of battery capacity during the degradation test

TABLE I. The variation of the capacity for the five cells

Cell NO.	Initial Capacity (Ah)	Final Capacity (Ah)
1	2.5743	2.1723
2	2.5629	2.3326
3	2.4028	1.9231
4	2.4425	1.9525
5	2.4627	1.9923

the red diamonds in Fig. 10. It is easily found from the distribution of the red diamonds in Fig. 10 that the distribution of the solutions endows the weak learners with diversity. Each solution contains information about the STFs and the hyperparameters setting of SVR, which can be further used to establish a weak learner.

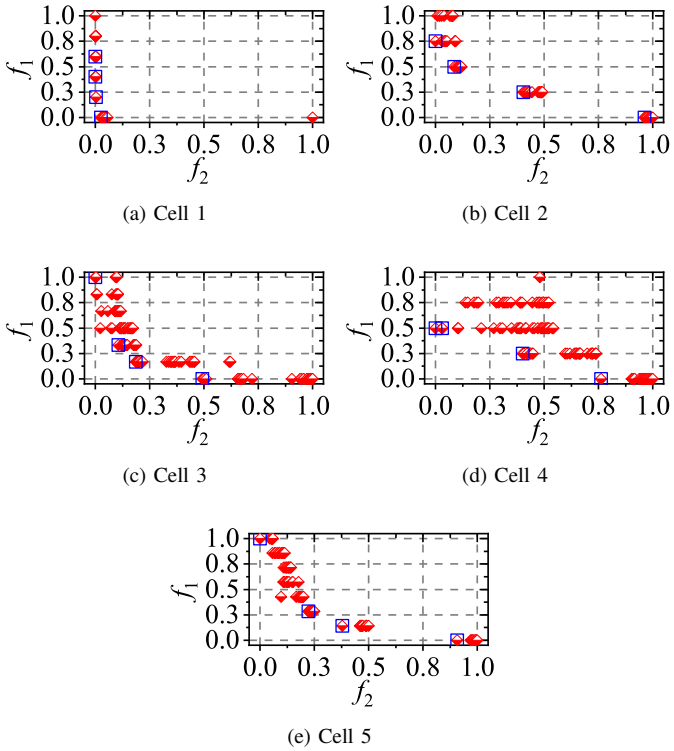

(a) Cell 1 (b) Cell 2

(c) Cell 3 (d) Cell 4

(e) Cell 5

Fig. 10. The non-dominated solutions from KnEA

Afterwards, the representative solutions can be picked up by PFSS. Generally, the solutions close to the origin of the coordinate are a good balance of the two cost functions in MOP. From Fig. 10, we can find that the non-dominated solutions (red diamonds) can be distributed into several groups. If all the non-dominated solutions are used to establish the weak learners, the structure of the ensemble framework will be exceeded. For both the efficiency and the accuracy, PFSS is designed to simplify the structure and choose a few representative solutions for an optimized weak learner formulation. Regarding the shape of the Pareto front in Fig. 10, 4 typical solutions are suitable for most cells. According to [40], we also calculate the Pure Diversity (PD) to quantitatively evaluate the diversity of the solutions selected by PFSS. The PD values of the 5 cells in Fig. 11 are 114.66, 827.32, 635.64, 927.72, and 855.86, which proves the effectiveness of PFSS. Thus, the 4 blue boxes in Fig. 10 selected by PFSS are used to formulate the weak learners with good diversity in this work. In this way, PFSS keeps the diversity and reduces the complexity of the whole ensemble structure simultaneously.

B. Validation of the proposed method in Case 1

From Fig. 1, we can find that the current pulses are performed at 18 different conditions. 18 weak learners can be naturally obtained, and the STFs from each condition endows the weak learner with diversity to some extent. Thus, an ensemble framework utilizing 18 weak learners [41] is chosen as a comparison method for the purpose of showing the advantages of the proposed method including a superior weak learner formulation procedure. The comparison method [41] is named as Method 1 in the following description. An obvious difference between the proposed method and Method 1 is that there is no specially designed weak learner formulation procedure in Method 1. In order to show the advantages of the SVR based method, the proposed method is also compared with ELM and GPR used in [16], [21]. For ELM the Sine function is used as an activation function and the number of the hidden nodes is set to 20. For GPR, rational quadratic function is selected as the kernel function. These configurations are carefully tuned to make a fair comparison.

This subsection validates the proposed method in Case 1. We have to point out here that all the tests of the SOH estimation methods in this work are based on 5-fold cross-validation as shown in Fig. 11. In step 1, the dataset is randomly divided into 5 subsets. During step 2, 4 subsets are used to train the model and the 1 left is used for testing. The validation will repeat 5 times until traversing all the subsets. The test results are then obtained in step 3. Thus, the validation results can ensure the generalization of the SOH estimation in this work.

The SOH estimation results in Case 1 are shown in Fig. 12. The proposed method is close to the reference (red line) in most conditions for Cell 1, while larger errors exist in the other three methods. For Cell 2 in Fig. 12b, we can see similar results that the proposed method (blue line) is closer to the reference. Compared with the comparison methods, the proposed method presents a better estimation accuracy for

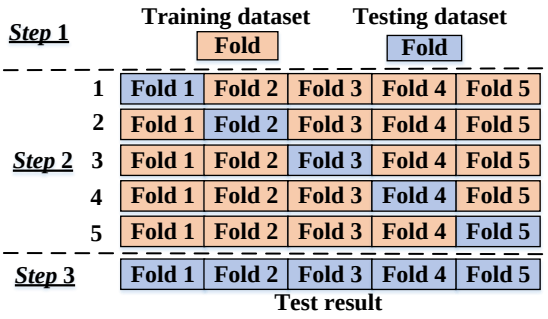

Fig. 11. The test procedure of estimation methods

both Cells 1 and 2. It is noted that Method 1 includes 18 weak learners, while the proposed method contains only 4 optimized weak learners. Thus, the proposed method is able to obtain accurate estimation results with fewer weak learners. The MOP and PFSS in the proposed method can maintain the diversity of the weak learner, thereby optimizing the weak learner formulation. The advantages of the proposed method are then proved.

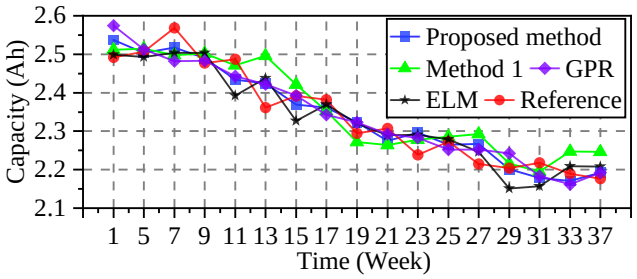

(a) Cell 1

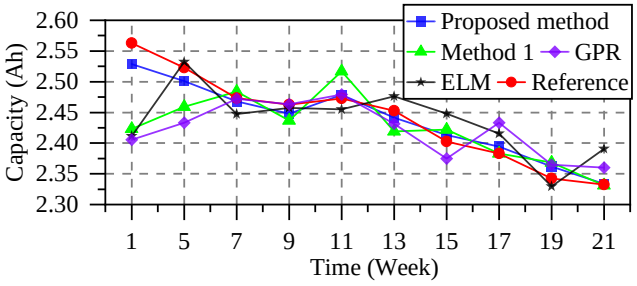

(b) Cell 2

Fig. 12. The estimation results of two LFP/C batteries in Case 1

We further analyze the estimation results by calculating the absolute error of the results in Fig. 12. The absolute errors of the three comparison methods are much larger than the usual error band in Fig. 13, which shows an unstable performance of those methods.

The Maximum Absolute Error (MAE) and Mean Squared Error (MSE) of the SOH estimation results are illustrated in Table. II. The accuracy of the estimation using the proposed method is much better than the other methods. The MAE of the proposed method is less than 35% of Method 1, while the

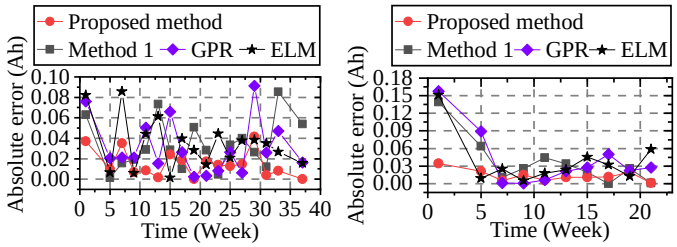

(a) Cell 1 (b) Cell 2

Fig. 13. The absolute error of two LFP/C batteries in Case 1

TABLE II. MAE and MSE of the SOH estimation methods in Case 1

Cell NO.	Error Type	ELM	GPR	Method 1	Proposed Method
Cell 1	MAE	0.0859	0.0913	0.0855	0.0417
	MSE	0.0018	0.0016	0.0017	3.7910×10^{-4}
Cell 2	MAE	0.1514	0.1574	0.1394	0.0344
	MSE	0.0031	0.0038	0.0028	2.6642×10^{-4}

TABLE III. MAE and MSE of the SOH estimation methods in Case 2

Cell NO.	Error Type	ELM	GPR	Method 1	Proposed Method
Cell 3	MAE	0.1175	0.1292	0.1287	0.0528
	MSE	0.0018	0.0015	0.0015	4.8847×10^{-4}
Cell 4	MAE	0.1424	0.1150	0.1253	0.0590
	MSE	0.0023	0.0016	0.0015	8.6598×10^{-4}
Cell 5	MAE	0.1503	0.1949	0.1641	0.0275
	MSE	0.0025	0.0021	0.0021	1.9835×10^{-4}

MSE is less than 15% of Method 1. In this way, the advantages of the proposed method are proved in Case 1.

C. Validation of the proposed method in Case 2

In this subsection, the SOH estimation methods are validated on Case 2, including Cells 3, 4, and 5. From Figs. 14 and 15, we can see the proposed method estimates the SOH with higher accuracy than the other methods. The MAE and MSE of the SOH estimation methods in Fig. 14 are summarized in Table. III. Both the error types of the proposed method are smaller than the three comparison methods, which proves the advantages of the proposed method in Case 2. It should be noted that KnEA, PFSS, SaDE and SVR training are both implemented in the training phase of the proposed method. Only 4 weak learners integrated by a group of weight coefficients are needed to be calculated for online estimation.

V. Conclusion

Considering the fact that one strong and unified data-driven estimator is difficult to be established in practice, this paper proposes a SOH estimation method by integrating a group of weak learners with STFs. An optimized formulation procedure, including PFSS and KnEA, is designed for the automatic initialization of weak learners with good diversity.

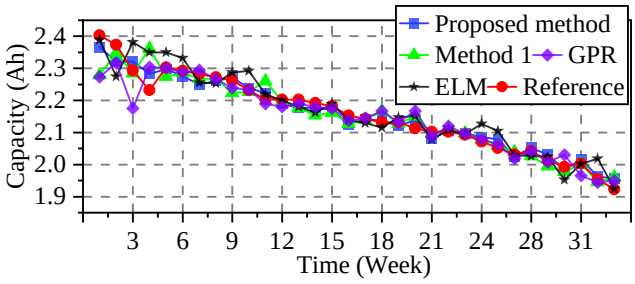

(a) Cell 3

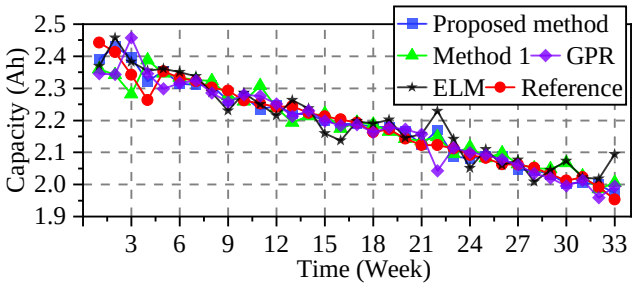

(b) Cell 4

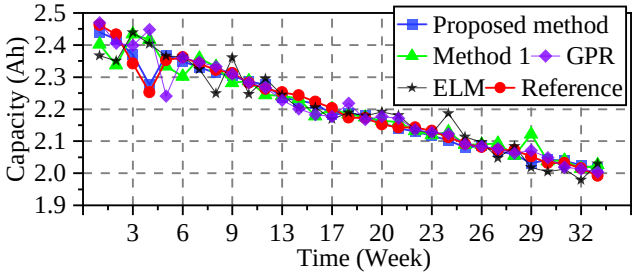

(c) Cell 5

Fig. 14. The estimation results of three LFP/C batteries in Case 2

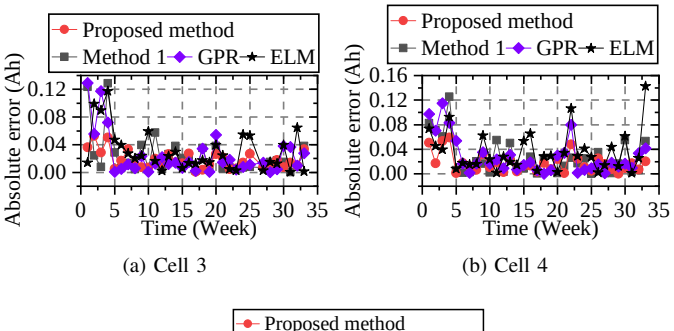

(a) Cell 3 (b) Cell 4

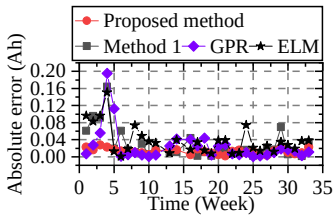

(c) Cell 5

Fig. 15. The absolute error of three LFP/C batteries in Case 2

According to the distribution of the non-dominated solutions in the Pareto front, weak learners can be well formulated. Afterwards, SaDE integrates weak learners to boost the overall performance of the SOH estimation. Note that the STF from a current pulse test, which is convenient to be obtained in real-life applications, can be used for Li-ion battery SOH estimation with good accuracy.

The proposed method, which uses only 4 weak learners, is validated on 5 LFP/C batteries aged under two different cycling profiles. In Case 1, the average MSE of the proposed method for Cells 1 and 2 is only 14.34% of Method 1 that includes 18 weak learners. In Case 2, the average MSE of the proposed method for Cells 3, 4, and 5 becomes 30.45% of Method 1. Note that all the estimation results in this work are validated by 5-fold cross-validation. Thus, the advantages of the proposed method, including an automatic weak learner formulation procedure, can be proved.

Since Li-ion battery generally presents a nonlinear degradation process, future works will focus on developing and validating this SOH estimation algorithm on a more sophisticated dataset.

REFERENCES

[1] Y. Yang, K. Hu, and C. Tsai, "Digital battery management design for point-of-load applications with cell balancing," *IEEE Transactions on Industrial Electronics*, vol. 67, no. 8, pp. 6365–6375, 2020.

[2] M. Rahman, A. Oni, E. Gemechu, and A. Kumar, "Assessment of energy storage technologies: A review," *Energy Conversion and Management*, vol. 223, p. 113295, 2020.

[3] A. Olabi, C. Onumaegbu, T. Wilberforce, M. Ramadan, M. Abdelkareem, and A. AI-Alami, "Critical review of energy storage systems," *Energy*, vol. 214, p. 118987, 2021.

[4] K. Liu, Y. Shang, Q. Ouyang, and W. D. Widanage, "A data-driven approach with uncertainty quantification for predicting future capacities and remaining useful life of lithium-ion battery," *IEEE Transactions on Industrial Electronics*, vol. 68, DOI 10.1109/TIE.2020.2973876, no. 4, pp. 3170–3180, 2021.

[5] K. Li, F. Wei, K. J. Tseng, and B. Soong, "A practical lithium-ion battery model for state of energy and voltage responses prediction incorporating temperature and ageing effects," *IEEE Transactions on Industrial Electronics*, vol. 65, no. 8, pp. 6696–6708, 2018.

[6] J. Meng, M. Ricco, G. Luo, M. Swierczynski, D.-I. Stroe, A.-I. Stroe, and R. Teodorescu, "An overview and comparison of online implementable soc estimation methods for lithium-ion battery," *IEEE Transactions on Industry Applications*, vol. 54, no. 2, pp. 1583–1591, 2017.

[7] J. Meng, G. Luo, M. Ricco, M. Swierczynski, D.-I. Stroe, and R. Teodorescu, "Overview of lithium-ion battery modeling methods for state-of-charge estimation in electrical vehicles," *Applied sciences*, vol. 8, no. 5, p. 659, 2018.

[8] K. Liu, X. Hu, H. Zhou, L. Tong, D. Widanalage, and J. Macro, "Feature analyses and modelling of lithium-ion batteries manufacturing based on random forest classification," *IEEE/ASME Transactions on Mechatronics*, DOI 10.1109/TMECH.2020.3049046, pp. 1–1, 2021.

[9] K. Liu, Z. Wei, Z. Yang, and K. Li, "Mass load prediction for lithium-ion battery electrode clean production: A machine learning approach," *Journal of Cleaner Production*, p. 125159, 2020.

[10] K. Bellache, M. B. Camara, B. Dakyo, and R. Sridhar, "Aging characterization of lithium iron phosphate batteries considering temperature and direct current undulations as degrading factors," *IEEE Transactions on Industrial Electronics*, DOI 10.1109/TIE.2020.3020021, pp. 1–1, 2020.

[11] S. Dey, Y. Shi, K. Smith, A. M. Colclasure, and X. Li, "From battery cell to electrodes: Real-time estimation of charge and health of individual battery electrodes," *IEEE Transactions on Industrial Electronics*, vol. 67, no. 3, pp. 2167–2175, 2020.

[12] B. Xu, A. Oudalov, A. Ulbig, G. Andersson, and D. S. Kirschen, "Modeling of lithium-ion battery degradation for cell life assessment," *IEEE Transactions on Smart Grid*, vol. 9, no. 2, pp. 1131–1140, 2016.

[13] S. Li, K. Li, E. Xiao, and C. Wong, "Joint soc and soh estimation for zinc nickel single flow batteries," *IEEE Transactions on Industrial Electronics*, vol. 67, no. 10, pp. 8484–8494, 2020.

[14] W. Yan, B. Zhang, G. Zhao, S. Tang, G. Niu, and X. Wang, "A battery management system with a lebesgue-sampling-based extended kalman filter," *IEEE Transactions on Industrial Electronics*, vol. 66, no. 4, pp. 3227–3236, 2019.

[15] C. Lei, J. Meng, D.-I. Stroe, J. Peng, G. Luo, and R. Teodorescu, "Multi-objective optimization of data-driven model for lithium-ion battery soh estimation with short-term feature," *IEEE Transactions on Power Electronics*, 2020.

[16] K. Liu, Y. Li, X. Hu, M. Lucu, and W. D. Widanage, "Gaussian process regression with automatic relevance determination kernel for calendar aging prediction of lithium-ion batteries," *IEEE Transactions on Industrial Informatics*, vol. 16, no. 6, pp. 3767–3777, 2019.

[17] L. Cai, J. Meng, D.-I. Stroe, G. Luo, and R. Teodorescu, "An evolutionary framework for lithium-ion battery state of health estimation," *Journal of Power Sources*, vol. 412, pp. 615 – 622, 2019.

[18] S. B. Vilsen, S. K. K. ær, and D. I. Stroe, "Log-linear model for predicting the lithium-ion battery age based on resistance extraction from dynamic aging profiles," *IEEE Transactions on Industry Applications*, vol. 56, no. 6, pp. 6937–6948, 2020.

[19] K. Liu, T. Ashwin, X. Hu, M. Lucu, and W. Widanage, "An evaluation study of different modelling techniques for calendar ageing prediction of lithium-ion batteries," *Renewable and Sustainable Energy Reviews*, vol. 131, DOI https://doi.org/10.1016/j.rser.2020.110017, p. 110017, 2020.

[20] Z. Wei, J. Zhao, R. Xiong, G. Dong, J. Pou, and K. J. Tseng, "Online estimation of power capacity with noise effect attenuation for lithium-ion battery," *IEEE Transactions on Industrial Electronics*, vol. 66, no. 7, pp. 5724–5735, 2019.

[21] H. Pan, Z. Lv, H. Wang, H. Wei, and L. Chen, "Novel battery state-of-health online estimation method using multiple health indicators and an extreme learning machine," *Energy*, vol. 160, pp. 466–477, 2018.

[22] K. Liu, X. Hu, Z. Wei, Y. Li, and Y. Jiang, "Modified gaussian process regression models for cyclic capacity prediction of lithium-ion batteries," *IEEE Transactions on Transportation Electrification*, vol. 5, DOI 10.1109/TTE.2019.2944802, no. 4, pp. 1225–1236, 2019.

[23] J. Meng, L. Cai, G. Luo, D.-I. Stroe, and R. Teodorescu, "Lithium-ion battery state of health estimation with short-term current pulse test and support vector machine," *Microelectronics Reliability*, vol. 88, pp. 1216–1220, 2018.

[24] X. Sui, S. He, J. Meng, R. Teodorescu, and D. I. Stroe, "Fuzzy entropy-based state of health estimation for li-ion batteries," *IEEE Journal of Emerging and Selected Topics in Power Electronics*, DOI 10.1109/JESTPE.2020.3047004, pp. 1–1, 2020.

[25] H. Dai, G. Zhao, M. Lin, J. Wu, and G. Zheng, "A novel estimation method for the state of health of lithium-ion battery using prior knowledge-based neural network and markov chain," *IEEE Transactions on Industrial Electronics*, vol. 66, no. 10, pp. 7706–7716, 2018.

[26] Y. Tan and G. Zhao, "Transfer learning with long short-term memory network for state-of-health prediction of lithium-ion batteries," *IEEE Transactions on Industrial Electronics*, vol. 67, no. 10, pp. 8723–8731, 2020.

[27] D.-I. Stroe and E. Schaltz, "Lithium-ion battery state-of-health estimation using the incremental capacity analysis technique," *IEEE Transactions on Industry Applications*, vol. 56, no. 1, pp. 678–685, 2019.

[28] E. Schaltz, D. I. Stroe, K. Nrregaard, L. S. Ingvardsen, and A. Christensen, "Incremental capacity analysis applied on electric vehicles for battery state-of-health estimation," *IEEE Transactions on Industry Applications*, DOI 10.1109/TIA.2021.3052454, pp. 1–1, 2021.

[29] J. Zhu, M. S. D. Darma, M. Knapp, D. R. Sorensen, M. Heere, Q. Fang, X. Wang, H. Dai, L. Mereacre, A. Senyshyn, X. Wei, and H. Ehrenberg, "Investigation of lithium-ion battery degradation mechanisms by combining differential voltage analysis and alternating current impedance," *Journal of Power Sources*, vol. 448, p. 227575, 2020.

[30] S. Zhang, X. Guo, X. Dou, and X. Zhang, "A rapid online calculation method for state of health of lithium-ion battery based on coulomb counting method and differential voltage analysis," *Journal of Power Sources*, vol. 479, p. 228740, 2020.

[31] M. Dubarry, C. Truchot, and B. Y. Liaw, "Synthesize battery degradation modes via a diagnostic and prognostic model," *Journal of power sources*, vol. 219, pp. 204–216, 2012.

[32] X. Feng, C. Weng, X. He, X. Han, L. Lu, D. Ren, and M. Ouyang, "Online state-of-health estimation for li-ion battery using partial charging segment based on support vector machine," *IEEE Transactions on Vehicular Technology*, vol. 68, no. 9, pp. 8583–8592, 2019.

[33] J. Meng, L. Cai, D.-I. Stroe, G. Luo, X. Sui, and R. Teodorescu, "Lithium-ion battery state-of-health estimation in electric vehicle using optimized partial charging voltage profiles," *Energy*, vol. 185, pp. 1054–1062, 2019.
[34] P. Guo, Z. Cheng, and L. Yang, "A data-driven remaining capacity estimation approach for lithium-ion batteries based on charging health feature extraction," *Journal of Power Sources*, vol. 412, pp. 442–450, 2019.
[35] M.-F. Ng, J. Zhao, Q. Yan, G. J. Conduit, and Z. W. Seh, "Predicting the state of charge and health of batteries using data-driven machine learning," *Nature Machine Intelligence*, pp. 1–10, 2020.
[36] K. A. Severson, P. M. Attia, N. Jin, N. Perkins, B. Jiang, Z. Yang, M. H. Chen, M. Aykol, P. K. Herring, D. Fraggedakis *et al.*, "Data-driven prediction of battery cycle life before capacity degradation," *Nature Energy*, vol. 4, no. 5, pp. 383–391, 2019.
[37] Z.-H. Zhou, *Ensemble methods: foundations and algorithms*. CRC press, 2012.
[38] X. Zhang, Y. Tian, and Y. Jin, "A knee point-driven evolutionary algorithm for many-objective optimization," *IEEE Transactions on Evolutionary Computation*, vol. 19, no. 6, pp. 761–776, 2014.
[39] A. K. Qin, V. L. Huang, and P. N. Suganthan, "Differential evolution algorithm with strategy adaptation for global numerical optimization," *IEEE transactions on Evolutionary Computation*, vol. 13, no. 2, pp. 398–417, 2008.
[40] H. Wang, Y. Jin, and X. Yao, "Diversity assessment in many-objective optimization," *IEEE Transactions on Cybernetics*, vol. 47, DOI 10.1109/TCYB.2016.2550502, no. 6, pp. 1510–1522, 2017.
[41] J. Meng, L. Cai, D.-I. Stroe, J. Ma, G. Luo, and R. Teodorescu, "An optimized ensemble learning framework for lithium-ion battery state of health estimation in energy storage system," *Energy*, vol. 206, p. 118140, 2020.

Jinhao Meng (M'19) received the M.S. degree in control theory and control engineering and the Ph.D. degree in electrical engineering from Northwestern Polytechnical University (NPU), Xi'an, China, in 2013 and 2019, respectively. He was supported by the China Scholarship Council as a joint Ph.D. student with the Department of Energy Technology, Aalborg University, Aalborg, Denmark. He is currently an associate researcher in Sichuan University, Chengdu, China.

His research interests include battery modeling, battery states estimation, and energy management of battery energy storage system.

Lei Cai received the Ph.D degree from Northwestern Polytechnical University (NPU), Xi'an, China, in 2017. He was supported by the China Scholarship Council as a joint Ph.D. student with the School of Computer Science, University of Birmingham, Birmingham, U.K. He is currently a lecturer with the Faculty of Computer Science and Engineering, Xi'an University of Technology, Xi' an, China.

His current research interests include evolutionary computation, optimization, data-driven battery modeling, battery states estimation, and energy management.

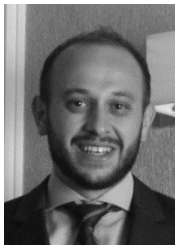

Daniel-Ioan Stroe (M'11) received the Dipl.Ing. degree in automatics from the Transilvania University of Brasov, Brasov, Romania, in 2008, and the M.Sc. degree in wind power systems and the Ph.D. degree in lifetime modelling of Lithium-ion batteries from Aalborg University, Aalborg, Denmark, in 2010 and 2014, respectively. He is currently an Assistant Professor with the Department of Energy Technology, Aalborg University. He was a Visiting Researcher at RWTH Aachen, Germany, in 2013. He has co-authored more than 70 journals and conference papers. His current research interests include energy storage systems for grid and e-mobility, Lithium-based batteries testing and modelling, and lifetime estimation of Lithium-ion batteries.

Xinrong Huang (S'20) received the M.S. degree in electrical engineering from Northwestern Polytechnical University (NPU), Xi'an, China, in 2018. She is supported by China Scholarship Council from 2018 to 2021 and currently working toward the Ph.D. degree in lifetime testing and modeling of Lithium-ion batteries at the Department of Energy Technology, Aalborg University, Aalborg, Denmark.

Her research interests include battery testing and modeling, battery charging strategies, and battery states estimation.

Jichang Peng received the B.S. degree in electrical engineering from North China University of Water Resources and Electric Power, Zhengzhou, China, in 2010, and the M.S. degree in control theory and control engineering and the Ph.D. degree in electrical engineering, both from Northwestern Polytechnical University, Xi'an, China, in 2013 and 2019, respectively.

He is currently a lecturer in Nanjing Institute of Technology, Nanjing, China.

His research interests include battery modeling, energy management, and aircraft starter/generator and sensorless control of brushless synchronous machines.

Tianqi Liu (SM'16) received the B.S. and the M.S. degrees from Sichuan University, Chengdu, China, in 1982 and 1986, respectively, and the Ph.D degree from Chongqing University, Chongqing, China, in 1996, all in electrical engineering.

She is currently a Professor with the College of Electrical Engineering, Sichuan University. Her research interests include power system analysis and stability control, HVDC, optimal operation, dynamic security analysis, dynamic state estimation, and load forecast.

Remus Teodorescu (F'12) received the Dipl.Ing. degree in electrical engineering from the Polytechnical University of Bucharest, Bucharest, Romania, in 1989, and the Ph.D. degree in power electronics from the University of Galati, Galati, Romania, in 1994. In 1998, he joined the Power Electronics Section, Department of Energy Technology, Aalborg University, Aalborg, Denmark, where he is currently a Full Professor. Since 2013, he has been a Visiting Professor with Chalmers University.

His research interests include design and control of grid-connected converters for photovoltaic and wind power systems, high voltage dc/flexible ac transmission systems based on modular multilevel converters, and storage systems based on Li-ion battery technology including modular converters and active battery management systems.